Metastability in high-entropy alloys: A review

As Published: 10.1557/JMR.2018.306

Publisher: Cambridge University Press (CUP)

Persistent URL: https://hdl.handle.net/1721.1/136346

Version: Author's final manuscript: final author's manuscript post peer review, without publisher's formatting or copy editing

REVIEW

This section of Journal of Materials Research is reserved for papers that are reviews of literature in a given area.

Metastability in high-entropy alloys: A review

Shaolou Wei[b)]
Department of Materials Science and Engineering, Massachusetts Institute of Technology, Cambridge, Massachusetts 02139, USA

Feng He[b)]
Department of Materials Science and Engineering, Massachusetts Institute of Technology, Cambridge, Massachusetts 02139, USA; and State Key Laboratory of Solidification Processing, Northwestern Polytechnical University, Xi'an 710072, People's Republic of China

Cemal Cem Tasan[a)]
Department of Materials Science and Engineering, Massachusetts Institute of Technology, Cambridge, Massachusetts 02139, USA

(Received 23 April 2018; accepted 6 August 2018)

Classical alloy design strategies often aim to benefit from metastability. Examples are numerous: metastable transformation- and twinning-induced plasticity steels, cobalt or titanium based alloys, age hardenable aluminum alloys, and severe plastic deformed nanostructured copper. In each of these cases, superior engineering property combinations are achieved by exploring limits of stability. For the case of high-entropy alloys (HEAs), on the other hand, majority of present research efforts focus on exploring compositions that would yield stable single-phase structures. HEA metastability and its effects on microstructure and property development constitute only a relatively small fraction of ongoing work. To help motivate and guide a corresponding shift in HEA research efforts, here in this paper, we provide an overview of the research activities on metastability in HEAs. To this end, we categorize the past research on the topic into two groups based on their focus, namely, compositional and structural stability, and discuss the most relevant and exciting findings.

I. INTRODUCTION

High-entropy alloys (HEAs), or compositionally complex alloys, have arguably become the fastest growing research direction in metallurgy in the last decade.[1–3] Majority of the research efforts in the initial part of this period focused on assessing the validity of the originally proposed HEA concept, i.e., configurational entropy-maximization can stabilize heavily alloyed single-phase solid solutions. While these proof-of-principle investigations have significantly contributed to the fundamentals of solid solution thermodynamics, the widely studied single-phase HEA microstructures are often not promising from the perspective of property requirements for engineering applications. It is known from decades of optimization of traditional alloy systems (e.g., Fe-, Al-, Ni-, and Ti-) that single-phase alloys can rarely exhibit competitive property combinations. In fact, exceptional toughness, ductility, and strength levels are usually achieved by utilizing different states of metastability.[4–7] Despite the apparent importance of metastability, research on metastability in HEAs has been developing rather slowly (Fig. 1) and still consists of a small fraction of HEA-related investigations (Fig. 1). The main goal of this paper is to provide an overview of the past work on metastability in HEAs, to help guide and motivate future research activities in this direction.

Comprehensive overviews of metastable states of alloys are provided in physical metallurgy textbooks.[8] While such a basic review need not be repeated here, the definition and classification of metastability are briefly presented for the sake of completeness. A "metastable" system, following the definition of the inventor of the terminology Ostwald,[9] persists in its existing state when undisturbed or subject to disturbances smaller than some small or infinitesimal amount, but passes to a more stable state when subject to greater disturbances. Using more thermodynamical terminology, such metastable states correspond to states which have excess free energy compared to that of equilibrium states. According to Turnbull,[10] three kinds of metastability can be identified, which would lead to the creation of such an excess free energy: morphological (arising from crystallographic

[a)]Address all correspondence to this author.
e-mail: tasan@mit.edu
[b)]These authors contributed equally to this work.
DOI: 10.1557/jmr.2018.306

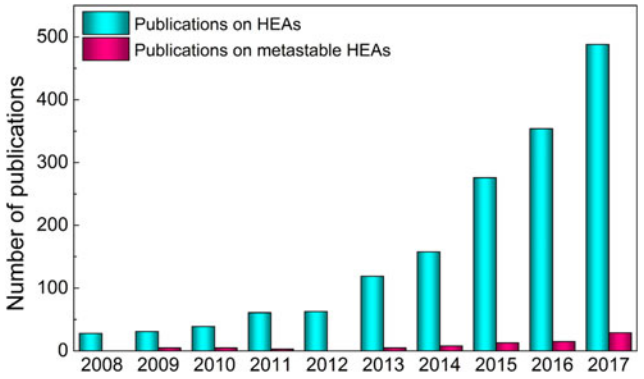

FIG. 1. Statistics for publications on HEAs and metastable HEAs in the recent decade (the total number of publications on HEAs was obtained from Web of Science and Scopus by the keyword "high-entropy alloys". Metastable HEAs were specified based on the following three criteria: (i) whether or not there exist an evident metastable-to-stable transition in composition or structure with respect to boundary conditions; (ii) whether or not such a transition has a significant influence on the HEAs' properties; and (iii) whether or not the HEAs are purposefully designed to be metastable. The number of publications on metastable HEAs was sorted out both manually and by adding constraint of "metastable" to the keyword).

defects), compositional (arising from extended solid solutions), and structural (arising from metastable phases). Often such effects present simultaneously since processing treatments that lead to metastability (e.g., quenching from elevated temperatures) generate multiple microstructural changes. In what follows, we discuss present findings on metastability in HEAs by specifically focusing on compositional and structural metastability. Excess free energy contributions from morphological effects are not discussed separately, although grain refinement and coarsening effects are discussed briefly as a subsection of the chapter on structural metastability.

II. COMPOSITIONAL METASTABILITY IN HEAS

The concept, HEA, was proposed based on the assumption that the high mixing entropy can assist compositionally complex alloys to form simple microstructure.[2] This concept is not initially restricted to single-phase solid solutions; however, numerous studies have been focused on finding stable single-phase solid solutions in the first decade since this concept was proposed.[3] The most widely studied single-phase HEAs are CoCrFeMnNi with face-centered cubic structure (FCC),[1] VNbMoTaW with body-centered cubic structure (BCC),[11] and HoDyYGdTb with hexagonal close packed structure (HCP).[12] The main argument for the phase stability of single-phase HEAs is that the high mixing entropy decreases the Gibbs free energy of the alloy systems according to $\Delta G_{\mathrm{mix}} = \Delta H_{\mathrm{mix}} - T\Delta S_{\mathrm{mix}}$.[13] Nevertheless, the effect of mixing entropy on the Gibbs free energy changes with temperature. The mixing entropy exhibits a significant contribution at elevated temperatures, while it plays less important role at medium or low temperatures. In addition, enthalpy also affects the phase stability of alloys and sometimes leads to phase separation even at high mixing entropy states.[14] In light of these two reasons, a series of work has been accomplished to clarify the phase stability mechanisms of single-phase HEAs and explore their metastable nature at medium and low temperatures. To summarize the temperature and composition-dependent metasatbility of HEAs, we first focus on two typical thermodynamically metastable phenomena: supersaturated solid solution and spinodal decomposition. Strategies of utilizing the metastability of HEAs are reviewed, and a brief discussion on the unique properties of precipitates within HEAs is also presented.

A. Spinodal decomposition

In 2004, Yeh et al.[2] reported the spinodal microstructure of disordered BCC and ordered BCC phase in Al_xCoCrCuFeNi HEAs. This spinodal decomposition results from the diminishing entropy stabilization effect at lower temperatures. Following Yeh's work, a series of work[15–23] has been carried out to characterize the effects of different elements on the microstructures and mechanical properties of the Al_xCoCrCuFeNi HEAs, but the spinodal decomposition in HEAs was not further illustrated. In 2015, Santodonato et al.[24] systematically investigated the structural evolution of the $Al_{1.3}$CoCrCuFeNi HEA by neutron diffraction and atom probe tomography (APT). They reported that the B2 phase transformed into a B2/BCC spinodal structure upon cooling. This decomposition occurred when the temperature was lower than 600 °C. Their APT and energy dispersive X-ray spectroscopy (EDS) results showed that the spinodal B2 phase composition was $Al_{1.3}Co_{0.79}Fe_{0.51}Ni$ while the spinodal BCC phase composition was $Co_{0.21}CrFe_{0.49}$. Similar spinodal decomposition was also found within the AlCoCrFeNi,[25] AlCrFeMnNi,[26] AlCoCrCuFeNi,[27,28] $Al_{0.5}$CoCrCuFeNi,[29] and $Al_{0.5}$CoCrFeNi[30] HEAs. Figure 2 shows a typical APT analysis of the decomposition within the AlCoCrCuFeNi HEA. The B2 phase regions (1 and 3) are rich in Ni and Al, while the BCC phase region (2) is rich in Cr and Fe. The HEA systems that show spinodal decomposition all consist of Al–Ni–Cr–Fe and the B2/BCC spinodal structure. The occurrence of the NiAl intermetallic compound (B2 structure) and Fe–Cr solid solution (BCC structure) has evidenced the governing role of enthalpy within these systems. HEAs synthesized from elements with significant difference in mixing enthalpy (such as Al–Ni and Fe–Cr) are prone to undergo such decomposition.[28] The spinodal decomposition characteristics of HEAs enable a remarkable potential for magnetic HEA design.

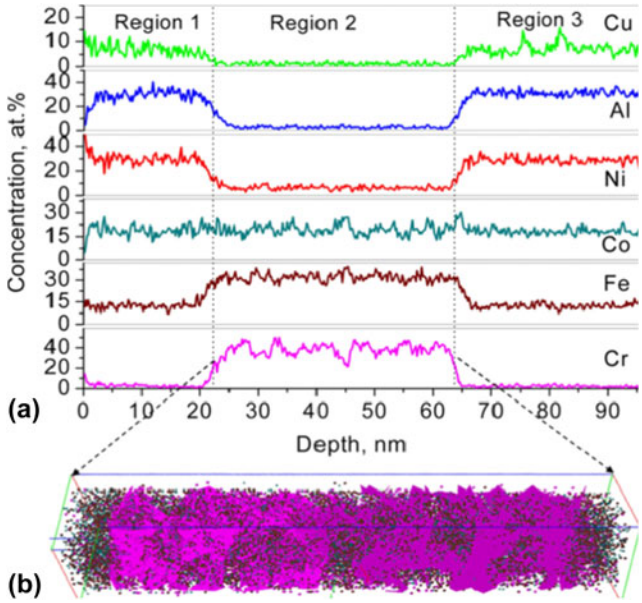

FIG. 2. (a) Concentration depth profiles of all alloying elements in the as-cast AlCoCrCuFeNi HEA (analyzed volume 9.5 × 9.5 × 93 nm^3); (b) atom clusters containing more than 30 at.% Fe and 20 at.% Co are superimposed on the iso-surface defined by 42 at.% Cr in region 2 (6.2 × 6.2 × 46 nm^3). Dots represent the positions of individual atoms.[27] Reprinted with permission from Ref. 27.

B. Supersaturated solid solutions

The first high-entropy solid solution CoCrFeMnNi was officially reported in 2004 by Cantor et al.[1] and was subsequently proved to possess excellent fracture toughness, high strength, and superior ductility even at cryogenic temperatures.[31,32] In the past decade, a wide range of high-entropy systems has been developed to find single-phase solid solution and address the phase selection rule of the single-phase HEAs.[13,33–35] However, most HEAs still consist of complex microstructures and only very few single-phase high-entropy systems, i.e., CoCrFeMnNi,[1] VNbMoTaW,[11] and HoDyYGdTb,[12] were found. In 2013, Otto et al.[14] designed a series of experiments to investigate the effects of enthalpy and entropy on the phase stability of HEAs. Their results highlighted the significant contribution of enthalpy and nonconfigurational entropy to phase stability of HEAs. The configurational entropy only dominates the mixing Gibbs free energy in ideal cases, where the alloy is single-phase and rigorously yields the ideal solution postulate. Following this idea, the phase stability of single-phase HEAs, i.e., CoCrFeMnNi HEA, has been proved to vary once temperature decreases because of the temperature-dependent contribution of mixing entropy to total Gibbs free energy. In 2016, almost at the same time, Pickering et al.[36] and Otto et al.[37] reported that the CoCrFeMnNi HEA decomposed after long-period annealing at intermediate temperatures. Figure 3 shows the microstructure, EDS mapping, and selected area electron diffraction (SAED) patterns of the CoCrFeMnNi HEA heat treated at 700 °C for 1000 h. A Cr-rich σ phase precipitates along the grain boundary (GB). At higher temperatures above 900 °C, the CoCrFeMnNi HEA displays single FCC structure, while at lower temperatures (500 °C), three different phases ($L1_0$-NiMn, B2-FeCo, and Cr-rich BCC phases) precipitate from the single-phase CoCrFeMnNi HEA. These two studies indicate that CoCrFeMnNi is a supersaturated solid solution at intermediate temperatures and will decompose after aging for sufficient time. Afterwards, He et al.[38] found the metastable nature of the CoCrFeNi HEA, and Stepanov et al.[39] reported the precipitation behavior in a typical single-phase BCC HfNbTaTiZr HEA. In addition, many other HEAs have been proved to exhibit single-phase structure at as-cast or homogenized states, while complex microstructures after annealing.[3,40,41] All these findings validate that the single-phase HEAs are supersaturated solid solution at low temperatures, which stimulates growing interest in precipitation-strengthened HEAs.

C. Precipitation-strengthened HEAs

Single-phase HEAs with FCC crystal structures possess superior ductility as well as fracture toughness, but unsatisfactory strength. Precipitation-strengthening is a relatively effective approach to enhance the strength of ductile materials. Based on the understanding of the metastability of the HEAs, researchers turned to strengthen FCC HEAs by precipitation. Although the enhanced properties of precipitation-strengthened HEAs may not be directly due to the metastability of the HEAs, the desired precipitates are obtained by taking advantage of the metastability. The precipitation-strengthened HEAs can be categorized into two groups according to the types of precipitates. The first group is coherent precipitates, such as the γ′ phase. The second group is intermetallic precipitates, such as the σ and the μ phases. A great amount of work has been accomplished towards precipitates within different HEA systems,[42–51] which greatly contributes to a better understanding of the alloying behavior of HEAs. While in the following discussion, we solely focus on research that intentionally made use of the metastability nature of HEAs.

Inspired by the design of commercial superalloys,[52] the γ′ phase was introduced into FCC HEAs.[53] The Al and Ti elements with appropriate contents were simultaneously introduced into the FCC matrix to obtain a supersaturated solid solution at high temperature and to achieve nanoscale γ′ particles by annealing at intermediate temperatures. The representative γ′-strengthened HEAs are $(CoCrFeNi)_{94}Al_4Ti_2$,[53] $(CoCrNi)_{94}Al_3Ti_3$,[54] and $Co_{1.5}CrFeNi_{1.5}Al_{0.2}Ti_{0.3}$[55] HEAs. The as-homogenized $(CoCrFeNi)_{94}Al_4Ti_2$ HEA exhibits a tensile strength of 500 MPa and an elongation

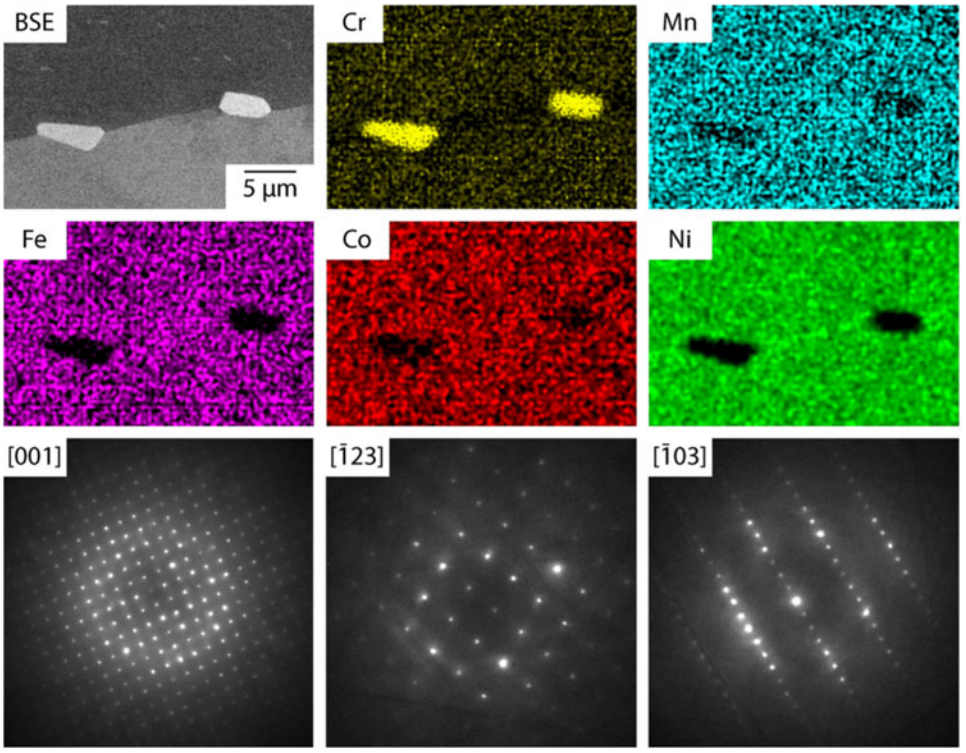

FIG. 3. Back scattered electron (BSE) image, EDS maps, and SAED patterns from the GB precipitate that appeared bright in BSE imaging in CrMnFeCoNi homogenized and then heat treated for 1000 h at 700 °C.[36] Reprinted with permission from Ref. 36 (CC BY 4.0: https://creativecommons.org/licenses/by/4.0/legalcode).

of 65%, while a better balance between strength (1100 MPa) and ductility (35%) was achieved by precipitation-strengthening. This HEA can be further strengthened by incorporating other strengthening mechanisms, such as dislocation strengthening. $(CoCrFeNi)_{94}Al_4Ti_2$ HEA is the first intentionally designed γ'-strengthened HEA and obtains superior compressive properties; however, the precipitation pathways within this HEA are relatively complex. Apart from the desirable nanosized γ' phase, a Ni_2Al-type $L2_1$ phase can also precipitate from the matrix as well. The $L2_1$ phase possesses a large particle size and distributes at the GB, resulting in a negative effect on the mechanical properties of $(CoCrFeNi)_{94}Al_xTi_y$ HEAs.[56]

A well-controlled γ'/γ microstructure was obtained in the $(CoCrNi)_{94}Al_3Ti_3$ HEA,[54] which exhibits a single FCC phase after solution treatment at elevated temperatures. This single-phase HEA becomes supersaturated solid solution as the temperature decreases. The nanoscale γ' phase is easily obtained by annealing this supersaturated solid solution at 800 °C for 1 h. It is noteworthy that the $L2_1$ phase dose not present in this HEA. The apparent distinction between the $(CoCrNi)_{94}Al_3Ti_3$ and $(CoCrFeNi)_{94}Al_4Ti_2$ HEAs results from the fact that Fe is excluded in the former one. Such a phenomenon suggests that fine optimization of Fe content is essential when designing the γ' phase in the CoCrFeNi-based HEAs. With the single γ'/γ microstructure, the $(CoCrNi)_{94}Al_3Ti_3$ HEA achieves an unprecedented increase of 70% in yield strength and 40% in tensile strength without sacrificing too much ductility. Interestingly, the γ' phase near GB in the $(CoCrNi)_{94}Al_3Ti_3$ HEA displays a plate-like shape, which is a typical sign of discontinuous precipitation. This factor has been well addressed in a recent publication.[57] Experimental analyses indicate that the chemical instability of supersaturated solid solution and GB excess energy both contribute to the formation of the plate-like precipitates. Such a phenomenon can be suppressed either through increasing gamma-prime solvus, or alleviating the mobility of grain boundaries.

The $Co_{1.5}CrFeNi_{1.5}Al_{0.2}Ti_{0.3}$ HEA was recently developed by Ming et al.[55] The size and shape of the γ' phase in this HEA were well controlled and the effect of γ' size on the mechanical properties was systematically investigated. An excellent chemical stability of supersaturated solid solution was obtained by a long-period solid solution heat treatment, which consequently avoided the formation of the plate-like γ' phase. The $L2_1$ phase was also effectively suppressed by decreasing the Fe and Cr content. The spherical γ' phase with a size of ~10 nm dispersedly precipitated from the supersaturated matrix and contributed to a dramatic precipitation-strengthening effect. The $Co_{1.5}CrFeNi_{1.5}Al_{0.2}Ti_{0.3}$ HEA with small-size

γ′ particles exhibits a yield strength of 750 MPa and an elongation of 40%. With increasing particle size, the ductility of the $Co_{1.5}CrFeNi_{1.5}Al_{0.2}Ti_{0.3}$ HEA decreases evidently. The inferior ductility associated with the long aging time is ascribed to the strong barrier of dislocation motion, where gliding dislocations can only bypass the interfacial precipitates by forming Orowan loops.

Strengthening HEAs by using intermetallic compounds is another novel approach. Intermetallic compounds were originally believed to be deteriorated to the ductility. Nevertheless, a good balance between strength (1200 MPa) and ductility (19%) was reported in the $CoCrFeNiMo_{0.3}$ HEA with σ and μ phases.[58] The σ and μ phases were obtained by annealing the supersaturated $CoCrFeNiMo_{0.3}$ HEA in 800–900 °C temperature range. The mechanism of intermetallic compound-strengthening is attributed to the fact that the FCC high-entropy matrix exhibits a significantly high work hardening exponent of 0.75 suppressing the propagation of microcracks at these brittle particles. Following this idea, the $Cr_{15}Fe_{20}Co_{35}Ni_{20}Mo_{10}$ HEA was developed.[59] By tuning the composition, a supersaturated solid solution with exceptional ductility and strain hardening capability has also been achieved. Optimizing thermal–mechanical processing condition has also been proved to enable the precipitation of intermetallic precipitates in the metastable $Cr_{15}Fe_{20}Co_{35}Ni_{20}Mo_{10}$ HEAs. With these precipitates in the ductile matrix, a high strength of 1410 MPa and a ductility of 12% were achieved.

D. High-entropy precipitates in the high-entropy matrix

Supersaturated solid solutions and precipitation-strengthening are both classical metallurgical phenomena in metallic materials; however, the high-entropy design gives rise to several novel and promising properties. Fig. 4 summarizes the mechanical properties of the single-phase, solid solution strengthened, coherent precipitates strengthened, and intermetallic precipitates strengthened HEAs. The effectiveness of the precipitation-strengthening is well demonstrated in Fig. 4. The single-phase HEAs show relatively high elongation with low strength. The additional alloying elements contribute to limited increasing strength mainly by solid solution strengthening. The precipitation-strengthened HEAs possess much higher strength than single-phase HEAs. Interestingly, some of the HEAs strengthened by intermetallic compounds are comparable with the coherent γ′-strengthened HEAs. Such unique behavior is owing to the superior work hardening capability of the FCC high-entropy matrix. In addition, FCC single-phase HEAs usually exhibit relatively low stacking fault energy.[32,60–62] This low stacking fault energy enables these HEAs to combine

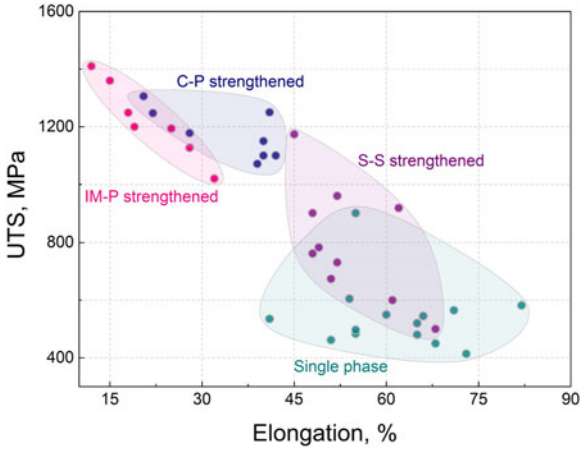

FIG. 4. The UTS versus elongation plot for single-phase, solid-solution (S-S) strengthened, coherent-precipitate (C-P) strengthened, and intermetallic-precipitate (IM-P) strengthened HEAs. Data were excerpted from Refs. 44, 53–55, 57–60, and 66.

deformation modules of dislocation glide, faulting, twinning, and deformation-induced phase transformation,[31,32,63–65] which contributes to an excellent work hardening capability. In particular, this also leads to the simultaneous enhancement of strength and ductility at cryogenic temperatures.[31,32] The exceptional work hardening capability of the high-entropy matrix enables a larger degree of freedom to design optimal precipitates.

Precipitates within HEAs also display complex chemical compositions. The APT results show that the Ni_3Al-type γ′ phase in HEAs consists of a large amount of Co, Ti, and relatively small amounts of Fe and Cr.[53,54,66] The Cr-rich σ phase within the CoCrFeNiMn HEAs also contains more than 50% of Co, Fe, Mn, and Ni.[37] It should be pointed out that these precipitates with complex chemical compositions also reflect the concept of high-entropy precipitates. The high-entropy precipitates within HEAs have been proved to possess unique properties compared to their conventional counterparts. For example, Zhao et al.[67] reported that the coarsening of the γ′ phase in the $(CoCrFeNi)_{94}Al_4Ti_2$ was much slower than that in the commercial Ni-based alloys. The γ′/γ antiphase boundary energy varies with additional alloying elements.[68] Zhao et al.[54] reported the antiphase boundary shearing behavior during deformation, which might result from the complex composition of the (Ni, Co, Cr)$_3$(Ti, Al) γ′ phase.

Precipitation-strengthened HEAs which combine the high-entropy matrix and the high-entropy precipitates exhibit promising potential for engineering applications. To make full use of these advantages of HEAs, developing new precipitation-strengthened HEAs with a matrix with low stacking fault energy and precipitates with tunable chemical compositions is suggested.

III. STRUCTURAL METASTABILITY IN HEAS

A. Polymorphism

The origination of the polymorphism study can be dated back to the 1900s, when Ostwald coined the postulate that almost any substance was able to exist in two or more phases if given the appropriate boundary conditions.[69] In materials science or condensed matter physics, polymorphism is referred to the occurrence of different crystal structures within a certain solid. The corresponded polymorphic transition is intrinsically a critical phenomenon that brings about the fluctuations in chemical, physical, and mechanical properties. From a thermodynamics point of view, the solid-state polymorphism phenomena can be classified into two categories: monotropic and enantiotropic transition.[69] In a monotropic system, the free energy curve of each polymorph will not intersect until the temperature reaches the highest melting point amongst all the polymorphs [Fig. 5(a)]. This indicates the irreversible nature of the transition that takes place below any melting point. On the contrary, in an enantiotropic system, free energy curves intersect below various melting points [Fig. 5(b)]. Such a characteristic implies the possibility to reversibly stabilize a certain polymorph by adjusting the boundary conditions. Nonetheless, the aforementioned two types of transitions share the common feature of evolving from a metastable state to a stable state, which results from the various stabilities of polymorphs.

Owing to the engineered configurational entropy, HEAs usually exhibit a high-symmetric single-phase structure.[3] These entropy-stabilized solid solution alloys were once believed to possess significant structural stability at elevated temperatures and extensive loads. The previously reviewed long period thermal stability investigations have evidenced the intrinsically metastable nature of a series of HEAs. Will these entropy-stabilized alloys always preserve one certain crystal structure even under extremely high pressure?

In light of this, a series of investigations have been accomplished in recent years focusing on the conventional CoCrNi-based FCC HEAs[70–74] [Fig. 6(a)] as well as rare-earth HEAs[72,75] [Fig. 6(b)]. As reported by Zhang et al.,[71] no significant structural transition was observed within the medium entropy CoCrNi alloy even under a hydrostatic pressure level of 50 GPa. When this basic alloy system is alloyed with Fe or Fe and Mn, the FCC to HCP polymorphic transition is detected to take place.[70,71] However, such a transition displays so sluggish characteristic that it does not complete even at around 40 GPa.[70,71] Polymorphic transition is not detected within either CoCrFeNiPd or AlCoCrCuFeNi alloy up to 50 GPa.[71,73] It should be noted that the volumetric response of the AlCoCrCuFeNi HEA displays a remarkable discrepancy from the trends of other HEAs summarized in this category. When it comes to rare earth HEAs, the situation is even more complex. The ReRuCoFe HEA possesses a relatively stable HCP structure with increasing pressure up to 60 GPa.[72] In contrast, the HoDyYGdTb HEA displays rather complex polymorphic transitions: it evolves from a conventional HCP structure through a Sm-type and a double HCP structure, then eventually ends up with a distorted FCC structure.[75]

Current opinions toward the mechanisms of polymorphic transitions within these HEAs vary with scales. In terms of atomic scale, Ma et al.[76] have validated that within the CoCrFeMnNi HEA, the HCP phase was thermodynamically more stable at lower temperature or under higher pressure compared to the FCC phase. Owing to the similar atomic packing characteristics between HCP and FCC structures, the HCP structure can be obtained by introducing layers of stacking faults within the FCC structure.[77–80] However, the kinetic energy barrier for the polymorphic

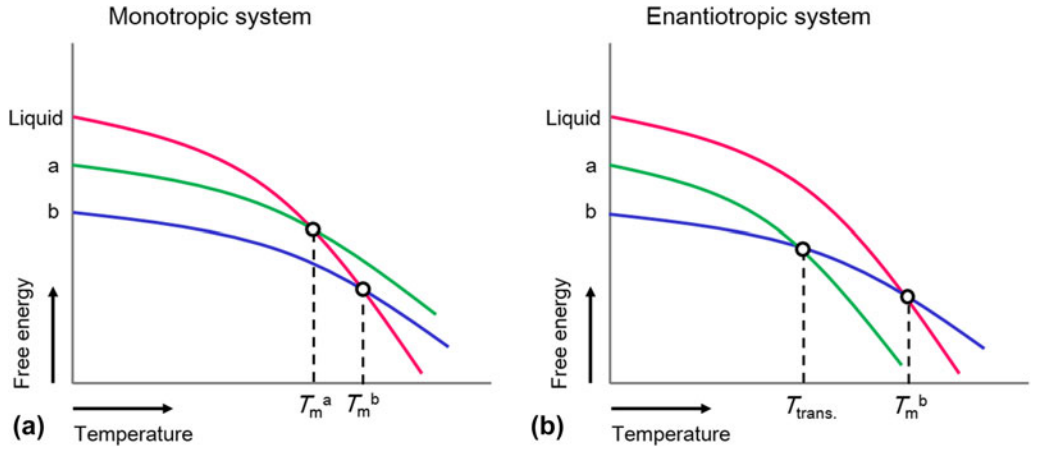

FIG. 5. A comparison between monotropic system (a) and enantiotropic system (b).

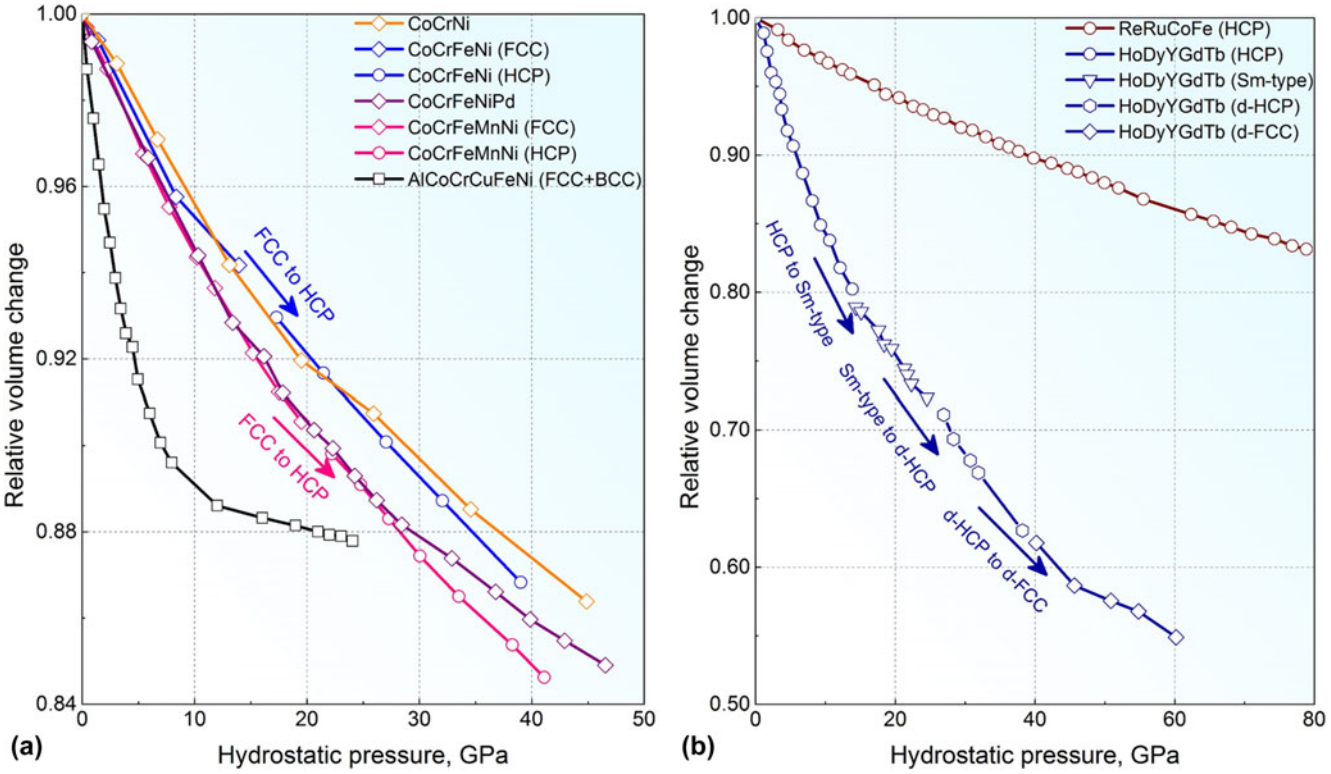

FIG. 6. A summary of recent investigations toward HEAs under high-pressure: (a) CoCrNi-based HEAs[70–74]; (b) rare-earth HEAs.[72,75]

transition of the CoCrFeMnNi HEA is remarkably high that it cannot be overcome unless the boundary conditions are varied to an extreme extent.[70] In other words, it is the high hydrostatic pressure that assists to overcome such an energy barrier, which facilities the FCC–HCP polymorphic transition. In the electronic scale, Yu et al.[75] addressed that the polymorphic transition of the HoDyYGdTb HEA was somehow linked with the d-band occupancy states. Owing to the high hydrostatic pressure, the s-d charge transfer within the heavily alloyed system brings about the increasing number of electrons in d-bands. This results in the variation of the bonding characteristics, which in turn accounts for the sequential polymorphic transition. Nonetheless, more quantitative mechanisms toward the correlation between the high-configurational entropy and the polymorphic transitions still remain to be investigated.

Apart from understanding the unique polymorphic transition mechanisms of HEAs, another intriguing fundamental issue is to construct the equation of state (EOS) for these heavily alloyed solids under high-pressure (namely, the pressure–volume relation). So far, limited work has been accomplished toward such a topic. The third order Birch–Murnaghan (M–B) equation has been widely applied to construct the EOS of compressed solids[81]:

$$p = \frac{3}{2}K_0\left[\left(\frac{V_p}{V_0}\right)^{-7/3} - \left(\frac{V_p}{V_0}\right)^{-5/3}\right]\left\{1 - \frac{3}{4}\left(4 - K_0'\right)\left[\left(\frac{V_p}{V_0}\right)^{-2/3} - 1\right]\right\} \quad , \qquad (1)$$

where p is the hydrostatic pressure, V_p and V_0 are the unit cell volume at a pressure level of p and zero, K_0 and K_0' represent the bulk modulus of the solid at zero pressure and the first pressure derivative. Under this configuration, Ahmad et al.[72] constructed the EOS for both the FCC-CoCrFeMnNi HEA and the HCP-ReRuCoFe HEA by regression analyses. A more general Bridgman equation can also be used to construct the EOS[82]:

$$\frac{V_p}{V_0} = \sum_{i=0}^{n} a_i^i p^i \quad , \qquad (2)$$

where p is the hydrostatic pressure, V_p and V_0 denote the unit cell volume at p and zero pressure, and a_i is the ith phenomenological parameter. Following the Bridgman's formalism, Li et al.[85] built the EOS for the BCC + FCC dual phase AlCoCrCuFeNi HEA.

Investigations toward polymorphic transitions within HEAs have validated the metastable nature of these

entropy-stabilized solid solution alloys. Apart from the temperature effects, more attention is suggested to be focused on understanding the metastability of HEAs with respect to high-pressure. Such effort will not only benefit the theoretical fundamentals but also contribute to a comprehensive metastability framework of HEAs under extreme circumstances.

B. Mechanically induced transformations in HEAs

Early research work on HEAs aimed at configurational entropy maximization, for the development of multicomponent, equiatomic alloys with single-phase solid solutions. Nonetheless, configurational entropy-based criteria alone cannot guarantee stability, as demonstrated by Otto et al. and others.[14,83] These observations led to the relaxation of the imposed compositional criteria for HEAs, and exploration of new compositional regimes, such as nonequiatomic HEAs[84,86] and HEAs with interstitial alloying elements.[87–90] Yao et al.[91] started from the equiatomic FeMnNiCoCr system to produce a nonequiatomic $Fe_{40}Mn_{27}Ni_{26}Co_5Cr_2$ (at.%) HEA and demonstrated that the resulting single-phase (FCC) solid solution similarly has high thermal and mechanical stability. Li et al.[88] and Wang et al.[87] demonstrated that carbon, despite being an interstitial alloying element, can be used in the FeMnNiCoCr and FeNiMnAlCr systems, to improve strength–ductility combinations.

These investigations and others alike motivated an important new design strategy for new HEAs. If single-phase solid solutions can be achieved in nonequiatomic alloys without sacrificing property benefits of HEAs (such as massive solid solution strengthening), composition modifications that would further reduce the single-phase stability can also be explored. This paved the way for the development of twinning-induced plasticity (TWIP) HEAs and transformation-induced plasticity (TRIP) HEAs.[91–94] In one of the pioneering studies of metastable HEAs, Li et al. demonstrated in the FeMnCoCr system that the Mn content can be modified to switch between dislocation-plasticity governed HEA, TWIP HEA, TRIP HEA, and a dual-phase TRIP HEA (Fig. 7).[93]

What is noteworthy in the design of metastable high-entropy dual-phase alloys is the reduction of both thermal and mechanical stability, to create the resulting microstructure and properties. In contrast to the equiatomic $Fe_{20}Mn_{20}Ni_{20}Co_{20}Cr_{20}$ (at.%) that develops a stable FCC structure upon cooling from the high temperature single-phase region, the nonequiatomic $Fe_{50}Mn_{30}Co_{10}Cr_{10}$ (at.%) system exhibits partial martensitic transformation to the HCP phase when quenching. This type of partial martensitic transformation during quenching is key in avoiding alloying element partitioning, i.e., development of high-entropy phases of identical chemical composition.[93,95]

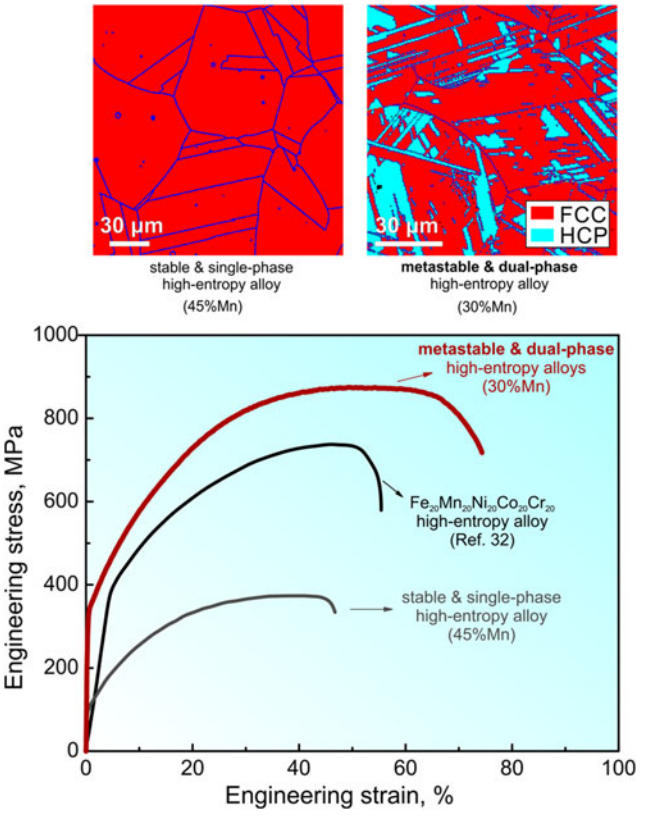

FIG. 7. By reducing Mn content, the stability of the matrix austenite phase can be reduced, leading to the formation of HCP both during quenching, and during mechanical testing. As a result, the achieved mechanical properties are superior to stable single-phase structures.

The metastable nature of the room temperature FCC phase leads to the mechanically induced martensitic transformation, and an increase of both ductility and strength. These mechanisms have been utilized by other researchers as well.[4,96]

Although metastable HEAs show improved property combinations compared to stable HEAs, their design has mostly been carried out based on high-throughput screening approaches, rather than by utilization computational predictions. An interesting work in the latter direction was of Ma et al., where predictive capabilities of the calculation of phase diagram (CALPHAD) approach was assessed for the equiatomic and nonequiatomic FeMnNiCoCr alloys.[97] The results demonstrated that systematic CALPHAD simulations can help predict equilibrium phase formation at high-temperatures or after nonequilibrium solidification processes, as well as some martensitic transformation effects.

C. Grain coarsening

Owing to the superior strength and excellent wear and fatigue resistance, nanocrystalline metals have stimulated extensive research interest compared to their bulk counterparts.[98] As one of the cost-effective methods to

achieve nanocrystalline structure in bulk metallic solids, severe plastic deformation (SPD) techniques, such as high-pressure torsion, heavy cold, and cryo-rolling (HCR) have been widely utilized to also fabricate nanostructured HEAs. An abundance of investigations have emerged in the literature focusing on microstructural characteristics, defect evolution as well as mechanical properties for HEAs after SPD.[99–109] A recent work by Bhattacharjee et al.[106] reported that the nanolamellar $AlCoCrFeNi_{2.1}$ HEA, which was achieved by cryo-rolling and annealing processes, exhibited a remarkable increase in both the yield strength and the ultimate tensile strength (UTS) without sacrificing too much ductility [Fig. 8(a)]. Such unique characteristics were mainly attributed to the formation of a hierarchical microstructure after SPD. Heczel et al.[108] quantified the defect evolution features such as dislocation density and twin-fault probability for an equiatomic CoCrFeMnNi HEA produced by HPT and successfully explained the enhanced mechanical properties. In the powder scale, mechanical alloying (MA) (often corresponded with various sintering techniques) is another viable approach to fabricate nanostructured bulk metallic solids.[110–113] In such processes, uniform solid solution phase is achieved owing to the high-energy mechanical milling. Fu et al.[113] reported a design of a nanostructured medium entropy TiFeCoNi alloy (MEA) via MA and spark plasma sintering (SPS) technique. This single FCC phase MEA displayed a unique multiscale grains characteristics with distinctively coarse grains (>1 μm) together with nanograins. They also confirmed that the nanostructured MEA kept a desirable balance between strength and ductility: with ultra-high compressive yield strength up to 1795 MPa and fracture strain of approximately 20% [Fig. 8(b)].

Even though the nanocrystalline HEAs produced by various SPD techniques have demonstrated superior mechanical properties, their intrinsically metastable nature still exhibits significant potential to drive the systems away from nanocrystallinity, bringing about grain coarsening even at ambient temperature. A series of studies have been reported in the literature aiming to examine the structural stability of HEAs after SPD.[114–117] In particular, Schuh et al.[114] investigated the microstructural and compositional evolution of a nanocrystalline CoCrFeMnNi HEA after HPT. They demonstrated that the mechanical properties underwent an unexpected softening response which was attributed to the interactions between structural and compositional metastability. Bhattacharjee et al.[117] and Liu et al.,[116] respectively, studied the grain coarsening kinetics of equiatomic CoCrFeMnNi HEA after HCR. As summarized in Fig. 9(a), the grain coarsening tendency exhibits a significant expedition as temperature rises beyond 800 °C. Liu et al.[116] also demonstrated that the grain coarsening kinetics yielded a power law of three with a nominal activation energy of 321.7 kJ/mol [Fig. 9(b)].

The aforementioned effort has systematically clarified the enhanced mechanical properties and the grain coarsening characteristics of HEAs after SPD. One fundamental question remains to be answered: would it be possible to employ the high-configurational entropy as a strategy to stabilize the nanocrystalline structure? In terms of thermodynamics, the Gibbs adsorption isotherm states

$$\mathrm{d}\gamma_{\mathrm{GB}} = S^{\mathrm{ex}}\mathrm{d}T - \sum_i \Gamma_i \mathrm{d}\mu_i \quad , \tag{3}$$

where γ_{GB} denotes the GB energy, S^{ex} is the excess entropy and the excess concentration at GB, Γ_i and μ_i

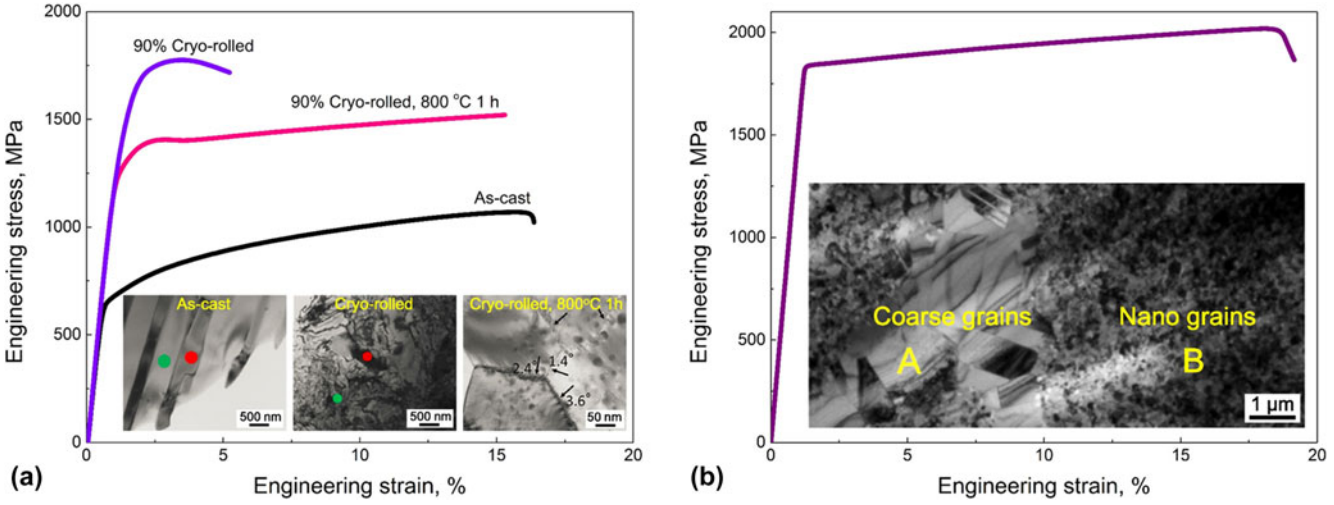

FIG. 8. Superior mechanical properties of nanocrystalline HEAs and MEAs: (a) Uniaxial tensile properties of nanolamellar HEAs produced by cryo-rolling[106]; (b) Uniaxial compressive properties of an MEA with multiscale grains fabricated by MA and SPS (regime A: coarse grains; regime B: nanograins).[113]

represent the excess solute quantity and the chemical potential of the *i*th element at GB. Within a saturated system, it is also recognized that the variation of GB energy with respect to temperature yields

$$\left(\frac{\partial \gamma_{\mathrm{GB}}}{\partial T}\right)_{p,X_i} \approx \left(\frac{\partial \gamma_{\mathrm{GB}}}{\partial T}\right)_{p,\mu_i} = -S^{\mathrm{ex}} \quad , \qquad (4)$$

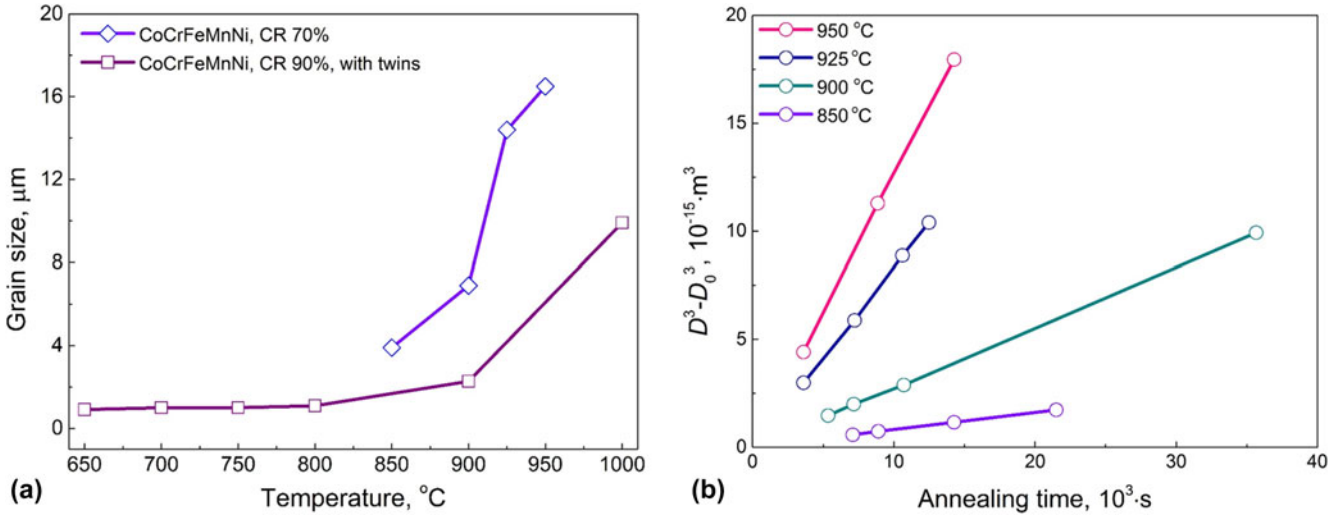

FIG. 9. Grain coarsening characteristics of CoCrFeMnNi HEAs after HPT: (a) grain size versus temperature[116,117]; (b) grain coarsening kinetics.[116]

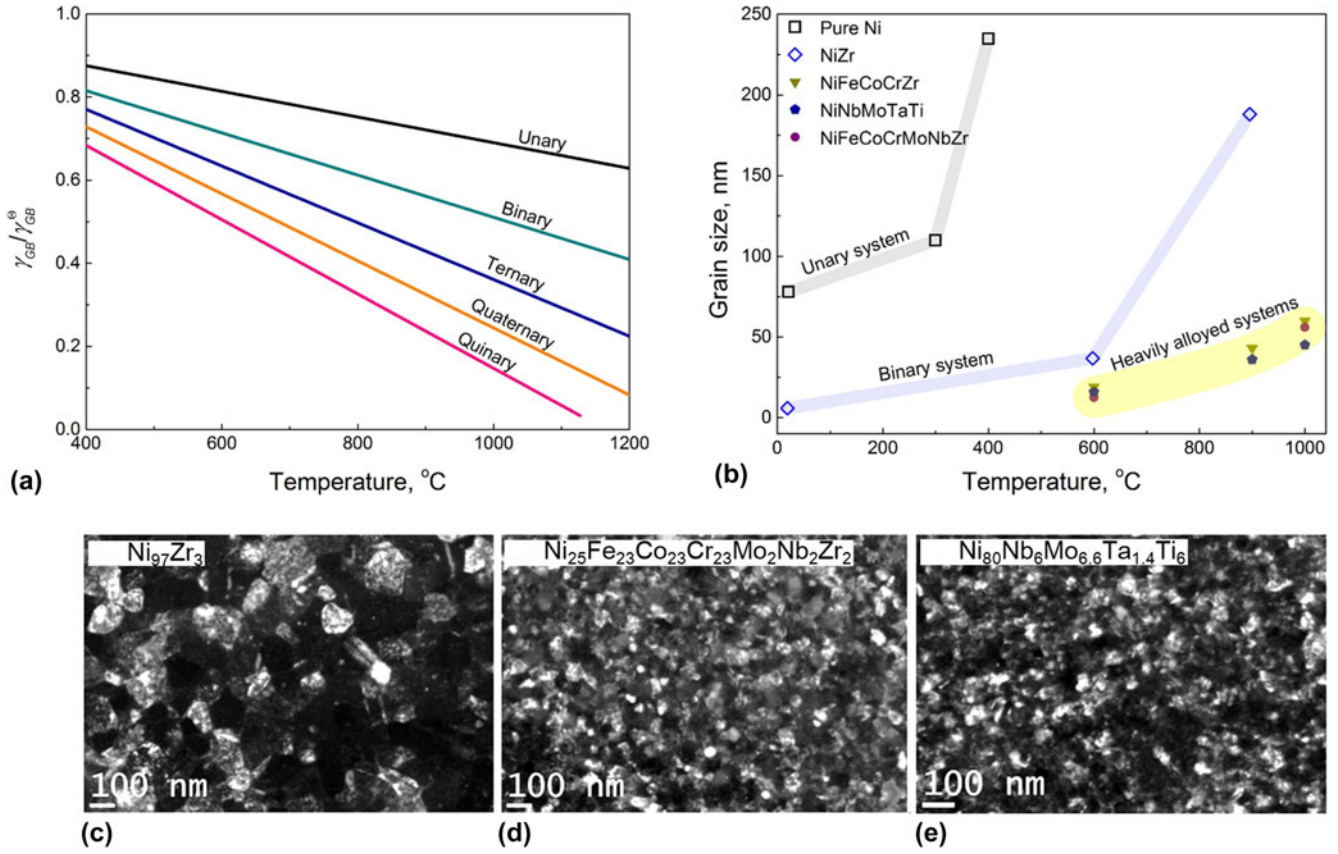

FIG. 10. Entropy as a strategy to stabilize nanograins[120]: (a) numerical experiments within hypothetical alloy systems; (b) grain size versus temperature of various alloys; (c)–(e) TEM dark-field images of selected alloys after annealing at 900 °C for 5 h. Reprinted with permission from Ref. 120.

therefore, the GB energy is theoretically feasible to be tuned down via a large positive excess entropy with increasing temperature. Considering an n component system, the GB energy can be expressed as[118]

$$\gamma_{GB} = \gamma_{GB}^{\Theta} - 2n\sum_{i\neq 0} X_{GB}^{i}\Delta H_{ads.} + 2n\sum_{i} k_B T X_{GB}^{i} \ln\left(\frac{X_{GB}^{i}}{X_{Bulk}^{i}}\right) + \gamma_{nonideal} \quad , \quad (5)$$

in which γ_{GB}^{Θ} is the reference state where there is no adsorption, X_{GB}^{i} and X_{Bulk}^{i} are the GB and bulk composition, $\Delta H_{ads.}$, T, k_B, and $\gamma_{nonideal}$ represent the adsorption enthalpy, temperature, Boltzmann constant, and nonideal correction term. In Eq. (5), the GB and bulk composition terms can be determined via the McLean–Langmuir equation[119]:

$$\ln\left(\frac{X_{GB}^{k}}{X_{Bulk}^{i}}\right) = \frac{X_{Bulk}^{k}}{X_{Bulk}^{i}}\exp\left(-\frac{\Delta H_{ads.}}{k_B T}\right) \quad . \quad (6)$$

Under this thermodynamic framework, Zhou et al.[120] performed a numerical experiment within a series of hypothetical alloy systems. As illustrated in Fig. 10(a), with increasing temperature, the ratio of GB energy to its reference state exhibits a linearly decreasing trend, which validates the aforementioned theory. Zhou et al.[120] further proved this concept by comparing the grain coarsening kinetics among nanocrystalline pure Ni, binary NiZr alloy, single-phase high-entropy NiFeCoCrZr, NiNbMoTaTi, and NiFeCoCrMoNbZr alloys. It is evident from the statistical data that the heavily alloyed systems display a remarkably sluggish grain growth kinetics.

Nanocrystalline HEAs fabricated by SPD methods have been proved to possess superior mechanical properties compared with their coarse-grain counterparts. Nonetheless, their metastable characteristics result in the grain coarsening tendency as temperature increases. The high-entropy concept has been proved theoretically and validated experimentally to be a potential strategy to overcome such a shortage.

IV. CONCLUSIONS

The past decade has witnessed the remarkable momentum of HEA research. In addition to existing research directions within the community, growing interest in metastable HEAs is expected to be continued. Under the metastable framework, future outlooks are briefly summarized as follows:

(1) The compositional metastability nature of HEAs enables a large degree of freedom for precipitation design. Making full use of the extensive solid solution strengthening and simultaneously incorporating various precipitates are suggested as promising strategies to balance strength and ductility at both ambient and elevated temperatures. In addition, much attention shall be directed to metastable HEAs with lower stacking fault energy.

(2) Nanocrystalline HEAs produced by various SPD techniques have been evidenced to exhibit exceptional mechanical performances. In a sense to alleviate the serious grain coarsening tendency, the high-entropy concept itself is also proposed as a potential strategy to further stabilize nanograins. Fundamental insights into tuning the defect structure, extending thermodynamic and kinetic theories to nondilute solution regimes still remain to be explored.

(3) The idea of phase transformation-induced plasticity in steel research has been successfully adapted to mechanically metastable HEA design. Such successful experiences also inspire a broader interpretation of the original high-entropy concept. To explore the wider world of nonequiatomic metastable HEAs, high throughput experimental and computational approaches are expected to be further developed.

ACKNOWLEDGMENTS

Shaolou Wei thanks Mr. Wujie Wang and Ms. Yuntong Zhu for fruitful discussions on chemical thermodynamics. Feng He is deeply indebted to the China Scholarship Council (CSC) for financial support.

REFERENCES

1. B. Cantor, I.T.H. Chang, P. Knight, and A.J.B. Vincent: Microstructural development in equiatomic multicomponent alloys. *Mater. Sci. Eng., A* **375–377**, 213 (2004).
2. J.W. Yeh, S.K. Chen, S.J. Lin, J.Y. Gan, T.S. Chin, T.T. Shun, C.H. Tsau, and S.Y. Chang: Nanostructured high-entropy alloys with multiple principal elements: Novel alloy design concepts and outcomes. *Adv. Eng. Mater.* **6**, 299 (2004).
3. D.B. Miracle and O.N. Senkov: A critical review of high entropy alloys and related concepts. *Acta Mater.* **122**, 448 (2017).
4. F.D. Fischer, G. Reisner, E. Werner, K. Tanaka, G. Cailletaud, and T. Antretter: A new view on transformation induced plasticity (TRIP). *Int. J. Plast.* **16**, 723 (2000).
5. M.E. Fine: Precipitation hardening of aluminum alloys. *Metall. Trans. A* **6**, 625 (1975).
6. T. Chookajorn, H.A. Murdoch, and C.A. Schuh: Design of stable nanocrystalline alloys. *Science* **337**, 951 (2012).
7. L. Lu, Y. Shen, X. Chen, L. Qian, and K. Lu: Ultrahigh strength and high electrical conductivity in copper. *Science* **304**, 422 (2004).
8. R.W. Cahn and P. Haasen: *Physical Metallurgy*, Vol. **1** (North-Holland, Amsterdam, 1996).
9. W. Ostwald: On chemical energy. *J. Am. Chem. Soc.* **15**, 421 (1893).
10. D. Turnbull: Metastable structures in metallurgy. *Metall. Trans. B* **12**, 217 (1981).
11. O. Senkov, G. Wilks, J. Scott, and D. Miracle: Mechanical properties of $Nb_{25}Mo_{25}Ta_{25}W_{25}$ and $V_{20}Nb_{20}Mo_{20}Ta_{20}W_{20}$ refractory high entropy alloys. *Intermetallics* **19**, 698 (2011).

12. A. Takeuchi, K. Amiya, T. Wada, K. Yubuta, and W. Zhang: High-entropy alloys with a hexagonal close-packed structure designed by equi-atomic alloy strategy and binary phase diagrams. *JOM* **66**, 1984 (2014).
13. Y. Zhang, T.T. Zuo, Z. Tang, M.C. Gao, K.A. Dahmen, P.K. Liaw, and Z.P. Lu: Microstructures and properties of high-entropy alloys. *Prog. Mater. Sci.* **61**, 1 (2014).
14. F. Otto, Y. Yang, H. Bei, and E.P. George: Relative effects of enthalpy and entropy on the phase stability of equiatomic high-entropy alloys. *Acta Mater.* **61**, 2628 (2013).
15. C-J. Tong, M-R. Chen, J-W. Yeh, S-J. Lin, S-K. Chen, T-T. Shun, and S-Y. Chang: Mechanical performance of the Al_xCoCrCuFeNi high-entropy alloy system with multiprincipal elements. *Metall. Mater. Trans. A* **36**, 1263 (2005).
16. C-J. Tong, Y-L. Chen, J-W. Yeh, S-J. Lin, S-K. Chen, T-T. Shun, C-H. Tsau, and S-Y. Chang: Microstructure characterization of Al_xCoCrCuFeNi high-entropy alloy system with multiprincipal elements. *Metall. Mater. Trans. A* **36**, 881 (2005).
17. H-Y. Chen, C-W. Tsai, C-C. Tung, J-W. Yeh, T-T. Shun, C-C. Yang, and S-K. Chen: Effect of the substitution of Co by Mn in Al-Cr-Cu-Fe-Co-Ni high-entropy alloys. *Ann. Chim.* **31**, 6 (2006).
18. M-R. Chen, S-J. Lin, J-W. Yeh, S-K. Chen, Y-S. Huang, and C-P. Tu: Microstructure and properties of $Al_{0.5}$CoCrCuFeNi-Ti_x (x = 0–2.0) high-entropy alloys *Mater. Trans.* **47**, 1395 (2006).
19. M-R. Chen, S-J. Lin, J-W. Yeh, M-H. Chuang, S-K. Chen, and Y-S. Huang: Effect of vanadium addition on the microstructure, hardness, and wear resistance of $Al_{0.5}$CoCrCuFeNi high-entropy alloy. *Metall. Mater. Trans. A* **37**, 1363 (2006).
20. J-M. Wu, S-J. Lin, J-W. Yeh, S-K. Chen, Y-S. Huang, and H-C. Chen: Adhesive wear behavior of Al_xCoCrCuFeNi high-entropy alloys as a function of aluminum content. *Wear* **261**, 513 (2006).
21. U.S. Hsu, U.D. Hung, J.W. Yeh, S.K. Chen, Y.S. Huang, and C.C. Yang: Alloying behavior of iron, gold and silver in AlCoCrCuNi-based equimolar high-entropy alloys. *Mater. Sci. Eng., A* **460–461**, 403 (2007).
22. Y-S. Huang, L. Chen, H-W. Lui, M-H. Cai, and J-W. Yeh: Microstructure, hardness, resistivity and thermal stability of sputtered oxide films of AlCoCrCu$_{0.5}$NiFe high-entropy alloy. *Mater. Sci. Eng., A* **457**, 77 (2007).
23. C-C. Tung, J-W. Yeh, T-t. Shun, S-K. Chen, Y-S. Huang, and H-C. Chen: On the elemental effect of AlCoCrCuFeNi high-entropy alloy system. *Mater. Lett.* **61**, 1 (2007).
24. L.J. Santodonato, Y. Zhang, M. Feygenson, C.M. Parish, M.C. Gao, R.J.K. Weber, J.C. Neuefeind, Z. Tang, and P.K. Liaw: Deviation from high-entropy configurations in the atomic distributions of a multi-principal-element alloy. *Nat. Commun.* **6**, 5964 (2015).
25. A. Manzoni, H. Daoud, R. Völkl, U. Glatzel, and N. Wanderka: Phase separation in equiatomic AlCoCrFeNi high-entropy alloy. *Ultramicroscopy* **132**, 212 (2013).
26. A. Munitz, L. Meshi, and M.J. Kaufman: Heat treatments' effects on the microstructure and mechanical properties of an equiatomic Al–Cr–Fe–Mn–Ni high entropy alloy. *Mater. Sci. Eng., A* **689**, 384 (2017).
27. S. Singh, N. Wanderka, K. Kiefer, K. Siemensmeyer, and J. Banhart: Effect of decomposition of the Cr–Fe–Co rich phase of AlCoCrCuFeNi high entropy alloy on magnetic properties. *Ultramicroscopy* **111**, 619 (2011).
28. S. Singh, N. Wanderka, B.S. Murty, U. Glatzel, and J. Banhart: Decomposition in multi-component AlCoCrCuFeNi high-entropy alloy. *Acta Mater.* **59**, 182 (2011).
29. X.D. Xu, P. Liu, S. Guo, A. Hirata, T. Fujita, T.G. Nieh, C.T. Liu, and M.W. Chen: Nanoscale phase separation in a fcc-based CoCrCuFeNiAl$_{0.5}$ high-entropy alloy. *Acta Mater.* **84**, 145 (2015).
30. K.E. Knipling, J.L. Tharpe, and P.K. Liaw: Nanoscale phase separation in $Al_{0.5}$CoCrFeNi(Cu) high entropy alloys as studied by atom probe tomography. *Microsc. Microanal.* **23**, 726 (2017).
31. F. Otto, A. Dlouhý, C. Somsen, H. Bei, G. Eggeler, and E.P. George: The influences of temperature and microstructure on the tensile properties of a CoCrFeMnNi high-entropy alloy. *Acta Mater.* **61**, 5743 (2013).
32. B. Gludovatz, A. Hohenwarter, D. Catoor, E.H. Chang, E.P. George, and R.O. Ritchie: A fracture-resistant high-entropy alloy for cryogenic applications. *Science* **345**, 1153 (2014).
33. J-W. Yeh, Y-L. Chen, S-J. Lin, and S-K Chen: High-entropy alloys—A new era of exploitation. *Mater. Sci. Forum.* **560** (2008).
34. Y. Zhang, Y.J. Zhou, J.P. Lin, G.L. Chen, and P.K. Liaw: Solid-solution phase formation rules for multi-component alloys. *Adv. Eng. Mater.* **10**, 534 (2008).
35. J-W. Yeh: Alloy design strategies and future trends in high-entropy alloys. *JOM* **65**, 1759 (2013).
36. E.J. Pickering, R. Muñoz-Moreno, H.J. Stone, and N.G. Jones: Precipitation in the equiatomic high-entropy alloy CrMnFeCoNi. *Scr. Mater.* **113**, 106 (2016).
37. F. Otto, A. Dlouhý, K.G. Pradeep, M. Kuběnová, D. Raabe, G. Eggeler, and E.P. George: Decomposition of the single-phase high-entropy alloy CrMnFeCoNi after prolonged anneals at intermediate temperatures. *Acta Mater.* **112**, 40 (2016).
38. F. He, Z. Wang, Q. Wu, J. Li, J. Wang, and C.T. Liu: Phase separation of metastable CoCrFeNi high entropy alloy at intermediate temperatures. *Scr. Mater.* **126**, 15 (2017).
39. N.D. Stepanov, N.Y. Yurchenko, S.V. Zherebtsov, M.A. Tikhonovsky, and G.A. Salishchev: Aging behavior of the HfNbTaTiZr high entropy alloy. *Mater. Lett.* **211**, 87 (2018).
40. Z. Wang, S. Guo, and C.T. Liu: Phase selection in high-entropy alloys: From nonequilibrium to equilibrium. *JOM* **66**, 1966 (2014).
41. J.C. Rao, H.Y. Diao, V. Ocelík, D. Vainchtein, C. Zhang, C. Kuo, Z. Tang, W. Guo, J.D. Poplawsky, Y. Zhou, P.K. Liaw, and J.T.M. De Hosson: Secondary phases in Al_xCoCrFeNi high-entropy alloys: An in situ TEM heating study and thermodynamic appraisal. *Acta Mater.* **131**, 206 (2017).
42. B. Gwalani, V. Soni, D. Choudhuri, M. Lee, J.Y. Hwang, S.J. Nam, H. Ryu, S.H. Hong, and R. Banerjee: Stability of ordered $L1_2$ and B_2 precipitates in face centered cubic based high entropy alloys—$Al_{0.3}$CoFeCrNi and $Al_{0.3}$CuFeCrNi$_2$. *Scr. Mater.* **123**, 130 (2016).
43. L. Zhang, Y. Zhou, X. Jin, X. Du, and B. Li: The microstructure and high-temperature properties of novel nano precipitation-hardened face centered cubic high-entropy superalloys. *Scr. Mater.* **146**, 226 (2018).
44. Y.L. Zhao, T. Yang, J.H. Zhu, D. Chen, Y. Yang, A. Hu, C.T. Liu, and J.J. Kai: Development of high-strength Co-free high-entropy alloys hardened by nanosized precipitates. *Scr. Mater.* **148**, 51 (2018).
45. S. Antonov, M. Detrois, and S. Tin: Design of novel precipitate-strengthened Al–Co–Cr–Fe–Nb–Ni high-entropy superalloys. *Metall. Mater. Trans. A* **49**, 305 (2017).
46. Q. Tang, Y. Huang, H. Cheng, X. Liao, T.G. Langdon, and P. Dai: The effect of grain size on the annealing-induced phase transformation in an $Al_{0.3}$CoCrFeNi high entropy alloy. *Mater. Des.* **105**, 381 (2016).

47. T-T. Shun and Y-C. Du: Microstructure and tensile behaviors of FCC $Al_{0.3}$CoCrFeNi high entropy alloy. *J. Alloys Compd.* **479**, 157 (2009).
48. F. He, Z. Wang, Y. Li, Q. Wu, J. Li, J. Wang, and C.T. Liu: Kinetic ways of tailoring phases in high entropy alloys. *Sci. Rep.* **6**, 34628 (2016).
49. T-T. Shun, L-Y. Chang, and M-H. Shiu: Microstructure and mechanical properties of multiprincipal component CoCrFeNi-Mo_x alloys. *Mater. Charact.* **70**, 63 (2012).
50. F. He, Z. Wang, J. Wang, Q. Wu, D. Chen, B. Han, J. Li, J. Wang, and J.J. Kai: Abnormal γ″–ε phase transformation in the $CoCrFeNiNb_{0.25}$ high entropy alloy. *Scr. Mater.* **146**, 281 (2018).
51. T-T. Shun, C-H. Hung, and C-F. Lee: The effects of secondary elemental Mo or Ti addition in $Al_{0.3}$CoCrFeNi high-entropy alloy on age hardening at 700 °C. *J. Alloys Compd.* **495**, 55 (2010).
52. Z. Wang, Y. Huang, J. Wang, and C. Liu: Design of high entropy alloys based on the experience from commercial superalloys. *Philos. Mag. Lett.* **95**, 1 (2015). (ahead-of-print).
53. J.Y. He, H. Wang, H.L. Huang, X.D. Xu, M.W. Chen, Y. Wu, X.J. Liu, T.G. Nieh, K. An, and Z.P. Lu: A precipitation-hardened high-entropy alloy with outstanding tensile properties. *Acta Mater.* **102**, 187 (2016).
54. Y.L. Zhao, T. Yang, Y. Tong, J. Wang, J.H. Luan, Z.B. Jiao, D. Chen, Y. Yang, A. Hu, C.T. Liu, and J.J. Kai: Heterogeneous precipitation behavior and stacking-fault-mediated deformation in a CoCrNi-based medium-entropy alloy. *Acta Mater.* **138**, 72 (2017).
55. K. Ming, X. Bi, and J. Wang: Realizing strength-ductility combination of coarse-grained $Al_{0.2}Co_{1.5}CrFeNi_{1.5}Ti_{0.3}$ alloy via nano-sized, coherent precipitates. *Int. J. Plast.* **100**, 177 (2018).
56. J.Y. He, H. Wang, Y. Wu, X.J. Liu, H.H. Mao, T.G. Nieh, and Z.P. Lu: Precipitation behavior and its effects on tensile properties of FeCoNiCr high-entropy alloys. *Intermetallics* **79**, 41 (2016).
57. Y-J. Chang and A-C. Yeh: The formation of cellular precipitate and its effect on the tensile properties of a precipitation strengthened high entropy alloy. *Mater. Chem. Phys.* **210**, 111 (2018).
58. W.H. Liu, Z.P. Lu, J.Y. He, J.H. Luan, Z.J. Wang, B. Liu, Y. Liu, M.W. Chen, and C.T. Liu: Ductile CoCrFeNiMo$_x$ high entropy alloys strengthened by hard intermetallic phases. *Acta Mater.* **116**, 332 (2016).
59. K. Ming, X. Bi, and J. Wang: Precipitation strengthening of ductile $Cr_{15}Fe_{20}Co_{35}Ni_{20}Mo_{10}$ alloys. *Scr. Mater.* **137**, 88 (2017).
60. A.J. Zaddach, R.O. Scattergood, and C.C. Koch: Tensile properties of low-stacking fault energy high-entropy alloys. *Mater. Sci. Eng., A* **636**, 373 (2015).
61. S. Zhao, G.M. Stocks, and Y. Zhang: Stacking fault energies of face-centered cubic concentrated solid solution alloys. *Acta Mater.* **134**, 334 (2017).
62. Y.H. Zhang, Y. Zhuang, A. Hu, J.J. Kai, and C.T. Liu: The origin of negative stacking fault energies and nano-twin formation in face-centered cubic high entropy alloys. *Scr. Mater.* **130**, 96 (2017).
63. G. Laplanche, A. Kostka, C. Reinhart, J. Hunfeld, G. Eggeler, and E.P. George: Reasons for the superior mechanical properties of medium-entropy CrCoNi compared to high-entropy CrMnFeCoNi. *Acta Mater.* **128**, 292 (2017).
64. G. Laplanche, A. Kostka, O.M. Horst, G. Eggeler, and E.P. George: Microstructure evolution and critical stress for twinning in the CrMnFeCoNi high-entropy alloy. *Acta Mater.* **118**, 152 (2016).
65. J. Miao, C.E. Slone, T.M. Smith, C. Niu, H. Bei, M. Ghazisaeidi, G.M. Pharr, and M.J. Mills: The evolution of the deformation substructure in a Ni–Co–Cr equiatomic solid solution alloy. *Acta Mater.* **132**, 35 (2017).
66. B. Han, J. Wei, Y. Tong, D. Chen, Y. Zhao, J. Wang, F. He, T. Yang, C. Zhao, Y. Shimizu, K. Inoue, Y. Nagai, A. Hu, C.T. Liu, and J.J. Kai: Composition evolution of gamma prime nanoparticles in the Ti-doped CoFeCrNi high entropy alloy. *Scr. Mater.* **148**, 42 (2018).
67. Y.Y. Zhao, H.W. Chen, Z.P. Lu, and T.G. Nieh: Thermal stability and coarsening of coherent particles in a precipitation-hardened $(NiCoFeCr)_{94}Ti_2Al_4$ high-entropy alloy. *Acta Mater.* **147**, 184 (2018).
68. D.M. Dimiduk, A.W. Thompson, and J.C. Williams: The compositional dependence of antiphase-boundary energies and the mechanism of anomalous flow in Ni_3Al alloys. *Philos. Mag. A* **67**, 675 (1993).
69. E.H. Lee: A practical guide to pharmaceutical polymorph screening & selection. *Asian J. Pharm. Sci.* **9**, 163 (2014).
70. F. Zhang, Y. Wu, H. Lou, Z. Zeng, V.B. Prakapenka, E. Greenberg, Y. Ren, J. Yan, J.S. Okasinski, X. Liu, Y. Liu, Q. Zeng, and Z. Lu: Polymorphism in a high-entropy alloy. *Nat. Commun.* **8**, 15687 (2017).
71. F. Zhang, S. Zhao, K. Jin, H. Bei, D. Popov, C. Park, J.C. Neuefeind, W.J. Weber, and Y. Zhang: Pressure-induced fcc to hcp phase transition in Ni-based high entropy solid solution alloys. *Appl. Phys. Lett.* **110**, 011902 (2017).
72. A.S. Ahmad, Y. Su, S. Liu, K. Ståhl, Y. Wu, X. Hui, U. Ruett, O. Gutowski, K. Glazyrin, and H. Liermann: Structural stability of high entropy alloys under pressure and temperature. *J. Appl. Phys.* **121**, 235901 (2017).
73. G. Li, D. Xiao, P. Yu, L. Zhang, P.K. Liaw, Y. Li, and R. Liu: Equation of state of an AlCoCrCuFeNi high-entropy alloy. *JOM* **67**, 2310 (2015).
74. E-W. Huang, C-M. Lin, J. Jain, S.R. Shieh, C-P. Wang, Y-C. Chuang, Y-F. Liao, D-Z. Zhang, T. Huang, and T-N. Lam: Irreversible phase transformation in a CoCrFeMnNi high entropy alloy under hydrostatic compression. *Mater. Today Commun.* **14**, 10 (2018).
75. P. Yu, L. Zhang, J. Ning, M. Ma, X. Zhang, Y. Li, P. Liaw, G. Li, and R. Liu: Pressure-induced phase transitions in HoDyYGdTb high-entropy alloy. *Mater. Lett.* **196**, 137 (2017).
76. D. Ma, B. Grabowski, F. Körmann, J. Neugebauer, and D. Raabe: Ab initio thermodynamics of the CoCrFeMnNi high entropy alloy: Importance of entropy contributions beyond the configurational one. *Acta Mater.* **100**, 90 (2015).
77. G. Olson and M. Cohen: Kinetics of nucleation strain-induced martensitic. *Metall. Mater. Trans. A* **6**, 791 (1975).
78. G. Olson and M. Cohen: A general mechanism of martensitic nucleation: Part I. General concepts and the FCC → HCP transformation. *Metall. Trans. A* **7**, 1897 (1976).
79. G. Olson and M. Cohen: A general mechanism of martensitic nucleation: Part II. FCC → BCC and other martensitic transformations. *Metall. Trans. A* **7**, 1905 (1976).
80. G. Olson and M. Cohen: A general mechanism of martensitic nucleation: Part III. Kinetics of martensitic nucleation. *Metall. Trans. A* **7**, 1915 (1976).
81. F. Birch: Finite strain isotherm and velocities for single-crystal and polycrystalline NaCl at high pressures and 300 K. *J. Geophys. Res.: Solid Earth* **83**, 1257 (1978).
82. P. Bridgman: *The Physics of High Pressure* (G. Bell and Sons, London, 1949). Google Scholar. 51 (1980).
83. O.N. Senkov, J.D. Miller, D.B. Miracle, and C. Woodward: Accelerated exploration of multi-principal element alloys with solid solution phases. *Nat. Commun.* **6**, 6529 (2015).
84. C.C. Tasan, Y. Deng, K.G. Pradeep, M.J. Yao, H. Springer, and D. Raabe: Composition dependence of phase stability, deformation mechanisms, and mechanical properties of the CoCrFeMnNi high-entropy alloy system. *JOM* **66**, 1993 (2014).

85. G. Li, D.H. Xiao, P.F. Yu, L.J. Zhang, P.K. Liaw, Y.C. Li, and R.P. Liu: Equation of state of an AlCoCrCuFeNi high-entropy alloy. *JOM*, **67**, 10 (2015).
86. K.G. Pradeep, C.C. Tasan, M.J. Yao, Y. Deng, H. Springer, and D. Raabe: Non-equiatomic high entropy alloys: Approach towards rapid alloy screening and property-oriented design. *Mater. Sci. Eng., A* **648**, 183 (2015).
87. Z. Wang, I. Baker, Z. Cai, S. Chen, J.D. Poplawsky, and W. Guo: The effect of interstitial carbon on the mechanical properties and dislocation substructure evolution in $Fe_{40.4}Ni_{11.3}Mn_{34.8}Al_{7.5}Cr_6$ high entropy alloys. *Acta Mater.* **120**, 228 (2016).
88. Z. Li, C.C. Tasan, H. Springer, B. Gault, and D. Raabe: Interstitial atoms enable joint twinning and transformation induced plasticity in strong and ductile high-entropy alloys. *Sci. Rep.* **7**, 40704 (2017).
89. L.B. Chen, R. Wei, K. Tang, J. Zhang, F. Jiang, L. He, and J. Sun: Heavy carbon alloyed FCC-structured high entropy alloy with excellent combination of strength and ductility. *Mater. Sci. Eng., A* **716**, 150 (2018).
90. Z. Wang, I. Baker, W. Guo, and J.D. Poplawsky: The effect of carbon on the microstructures, mechanical properties, and deformation mechanisms of thermo-mechanically treated $Fe_{40.4}Ni_{11.3}Mn_{34.8}Al_{7.5}Cr_6$ high entropy alloys. *Acta Mater.* **126**, 346 (2017).
91. M.J. Yao, K.G. Pradeep, C.C. Tasan, and D. Raabe: A novel, single phase, non-equiatomic FeMnNiCoCr high-entropy alloy with exceptional phase stability and tensile ductility. *Scr. Mater.* **72–73**, 5 (2014).
92. Y. Deng, C.C. Tasan, K.G. Pradeep, H. Springer, A. Kostka, and D. Raabe: Design of a twinning-induced plasticity high entropy alloy. *Acta Mater.* **94**, 124 (2015).
93. Z. Li, K.G. Pradeep, Y. Deng, D. Raabe, and C.C. Tasan: Metastable high-entropy dual-phase alloys overcome the strength-ductility trade-off. *Nature* **534**, 227 (2016).
94. Z.M. Li, C.C. Tasan, K.G. Pradeep, and D. Raabe: A TRIP-assisted dual-phase high-entropy alloy: Grain size and phase fraction effects on deformation behavior. *Acta Mater.* **131**, 323 (2017).
95. D. Raabe, C.C. Tasan, H. Springer, and M. Bausch: From high-entropy alloys to high-entropy steels. *Steel Res. Int.* **86**, 1127 (2015).
96. B.C. De Cooman, Y. Estrin, and S.K. Kim: Twinning-induced plasticity (TWIP) steels. *Acta Mater.* **142**, 283 (2018).
97. D. Ma, M. Yao, K.G. Pradeep, C.C. Tasan, H. Springer, and D. Raabe: Phase stability of non-equiatomic CoCrFeMnNi high entropy alloys. *Acta Mater.* **98**, 288 (2015).
98. A.J. Detor and C.A. Schuh: Microstructural evolution during the heat treatment of nanocrystalline alloys. *J. Mater. Res.* **22**, 3233 (2011).
99. N. Stepanov, N.Y. Yurchenko, A. Gridneva, S. Zherebtsov, Y.V. Ivanisenko, and G. Salishchev: Structure and hardness of B2 ordered refractory $AlNbTiVZr_{0.5}$ high entropy alloy after high-pressure torsion. *Mater. Sci. Eng., A* **716**, 308 (2018).
100. Q.H. Tang, Y. Huang, Y.Y. Huang, X.Z. Liao, T.G. Langdon, and P.Q. Dai: Hardening of an $Al_{0.3}CoCrFeNi$ high entropy alloy via high-pressure torsion and thermal annealing. *Mater. Lett.* **151**, 126 (2015).
101. I.S. Wani, T. Bhattacharjee, S. Sheikh, Y.P. Lu, S. Chatterjee, P.P. Bhattacharjee, S. Guo, and N. Tsuji: Ultrafine-Grained $AlCoCrFeNi_{2.1}$ eutectic high-entropy alloy. *Mater. Res. Lett.* **4**, 174 (2016).
102. S. Yoshida, T. Bhattacharjee, Y. Bai, and N. Tsuji: Friction stress and Hall–Petch relationship in CoCrNi equi-atomic medium entropy alloy processed by severe plastic deformation and subsequent annealing. *Scr. Mater.* **134**, 33 (2017).
103. K.B. Zhang, Z.Y. Fu, J.Y. Zhang, J. Shi, W.M. Wang, H. Wang, Y.C. Wang, and Q.J. Zhang: Nanocrystalline CoCrFeNiCuAl high-entropy solid solution synthesized by mechanical alloying. *J. Alloys Compd.* **485**, L31 (2009).
104. Y.H. Jo, S. Jung, W.M. Choi, S.S. Sohn, H.S. Kim, B.J. Lee, N.J. Kim, and S. Lee: Cryogenic strength improvement by utilizing room-temperature deformation twinning in a partially recrystallized VCrMnFeCoNi high-entropy alloy. *Nat. Commun.* **8**, 15719 (2017).
105. B. Schuh, B. Völker, V. Maier-Kiener, J. Todt, J. Li, and A. Hohenwarter: Phase decomposition of a single-phase AlTiVNb high-entropy alloy after severe plastic deformation and annealing. *Adv. Eng. Mater.* **19**, 1600674 (2017).
106. T. Bhattacharjee, I. Wani, S. Sheikh, I. Clark, T. Okawa, S. Guo, P. Bhattacharjee, and N. Tsuji: Simultaneous strength-ductility enhancement of a nano-lamellar $AlCoCrFeNi_{2.1}$ eutectic high entropy alloy by cryo-rolling and annealing. *Sci. Rep.* **8**, 3276 (2018).
107. H. Yuan, M-H. Tsai, G. Sha, F. Liu, Z. Horita, Y. Zhu, and J.T. Wang: Atomic-scale homogenization in an fcc-based high-entropy alloy via severe plastic deformation. *J. Alloys Compd.* **686**, 15 (2016).
108. A. Heczel, M. Kawasaki, J.L. Lábár, J-i. Jang, T.G. Langdon, and J. Gubicza: Defect structure and hardness in nanocrystalline CoCrFeMnNi high-entropy alloy processed by high-pressure torsion. *J. Alloys Compd.* **711**, 143 (2017).
109. W. Wu, S. Ni, Y. Liu, B. Liu, and M. Song: Amorphization at twin-twin intersected region in FeCoCrNi high-entropy alloy subjected to high-pressure torsion. *Mater. Charact.* **127**, 111 (2017).
110. C.S. babu, K. Sivaprasad, V. Muthupandi, and J.A. Szpunar: Characterization of nanocrystalline AlCoCrCuNiFeZn high entropy alloy produced by mechanical alloying. *Procedia Mater. Sci.* **5**, 1020 (2014).
111. Z. Fu, W. Chen, H. Xiao, L. Zhou, D. Zhu, and S. Yang: Fabrication and properties of nanocrystalline $Co_{0.5}FeNiCrTi_{0.5}$ high entropy alloy by MA–SPS technique. *Mater. Des.* **44**, 535 (2013).
112. S. Varalakshmi, M. Kamaraj, and B.S. Murty: Formation and stability of equiatomic and nonequiatomic nanocrystalline CuNiCoZnAlTi high-entropy alloys by mechanical alloying. *Metall. Mater. Trans. A* **41**, 2703 (2010).
113. Z. Fu, B.E. MacDonald, D. Zhang, B. Wu, W. Chen, J. Ivanisenko, H. Hahn, and E.J. Lavernia: Fcc nanostructured TiFeCoNi alloy with multi-scale grains and enhanced plasticity. *Scr. Mater.* **143**, 108 (2018).
114. B. Schuh, F. Mendez-Martin, B. Völker, E.P. George, H. Clemens, R. Pippan, and A. Hohenwarter: Mechanical properties, microstructure and thermal stability of a nanocrystalline CoCrFeMnNi high-entropy alloy after severe plastic deformation. *Acta Mater.* **96**, 258 (2015).
115. B. Schuh, B. Völker, J. Todt, N. Schell, L. Perrière, J. Li, J. Couzinié, and A. Hohenwarter: Thermodynamic instability of a nanocrystalline, single-phase TiZrNbHfTa alloy and its impact on the mechanical properties. *Acta Mater.* **142**, 201 (2018).
116. W.H. Liu, Y. Wu, J.Y. He, T.G. Nieh, and Z.P. Lu: Grain growth and the Hall–Petch relationship in a high-entropy FeCrNiCoMn alloy. *Scr. Mater.* **68**, 526 (2013).
117. P.P. Bhattacharjee, G.D. Sathiaraj, M. Zaid, J.R. Gatti, C. Lee, C-W. Tsai, and J-W. Yeh: Microstructure and texture evolution during annealing of equiatomic CoCrFeMnNi high-entropy alloy. *J. Alloys Compd.* **587**, 544 (2014).
118. P. Wynblatt and D. Chatain: Anisotropy of segregation at grain boundaries and surfaces. *Metall. Mater. Trans. A* **37**, 2595 (2006).
119. D. MacLean: *Grain Boundaries in Metals* (Clarendon Press, Oxford, London, 1957).
120. N. Zhou, T. Hu, J. Huang, and J. Luo: Stabilization of nanocrystalline alloys at high temperatures via utilizing high-entropy grain boundary complexions. *Scr. Mater.* **124**, 160 (2016).